Int. J. Microgravity Sci. Appl. 32 (2) 2015, 320211
DOI :10.15011/ijmsa.32.320211

IIIII Original Paper IIIII

Results of Microgravity Experiments Using the Balloon Operated Vehicle with a New Drag-Free Control Method

Masao KIKUCHI[1], Takehiko ISHIKAWA[1], Shin YAMAMOTO[2], Shujiro SAWAI[3], Yusuke MARU[3], Shinichiro SAKAI[3], Nobutaka BANDO[3], Shigehito SHIMIZU[3], Hiroaki KOBAYASHI[4], Tetsuo YOSHIMITSU[3], Yuji KAN[1], Takanari MIZUSHIMA[1], Seijiro FUKUYAMA[5], Junpei OKADA[1], Shinichi YODA[3], Hideyuki FUKE[3], Yuya KAKEHASHI[3] and Tatsuaki HASHIMOTO[3]

Abstract

A microgravity experiment system using a high altitude balloon has been developed. In order to accommodate payloads larger than previous system which employed three- dimensional drag-free control, one-dimensional drag-free control has been applied. The first test flight was conducted in Aug. 2014. A gravity level below 10^{-3} G was obtained for more than 30 seconds during the free-fall of the capsule. A combustion experiment was conducted during the low gravity condition.

Keyword(s): High altitude balloon, Free-fall, Drag-free control

Received 25 Dec. 2014, accepted 26 Feb. 2015, published 31 Apr. 2015

1. Introduction

The usefulness of the high-altitude balloon operated vehicle as a microgravity experiment method with high quality microgravity level was demonstrated by Hashimoto et al.[1-4]. It was shown that the experimental system could provide low-gravity environment in the order of 10^{-4} G for around 30 s by three-dimensional drag-free control which controls the gap between inner capsule (microgravity experimental section) and the outer capsule (the free falling vehicle) and keeps the inner capsule floating within the outer capsule. However, the maximum payload size was very limited in this system.

In order to enlarge the allowable payload size with sustaining microgravity level, a new drag-free control method was developed [5]. To demonstrate the technical capability of the new system, a flight experiment using a high-altitude balloon was conducted. The flight operations were performed at the JAXA's Taiki Aerospace Research Field (TARF), located in the town of Taiki in Hokkaido, in the summer of 2012. However, the flight experiment was postponed due to bad weather conditions. After additional postponements in 2013 and 2014, the flight experiment was finally performed in August 2014.

This paper briefly reports the outline of the experiment and presents the obtained gravity levels.

2. Overview of the Experiment

The primary objective of the flight experiment is to demonstrate and verify the new drag-free control system. As described in details later, the new system was designed to accommodate a payload whose size is as large as that of the European TEXUS sounding rocket. Since the experimental apparatus DCU (Droplet Array Combustion Unit) employed for microgravity experiments with TEXUS 46 in 2009 [6] was available, it was selected as the payload of this balloon experiment. The engineering model (EM) of the DCU was modified so that it met the flight operation of the balloon operated vehicle (BOV). It was also intended to obtain scientific data on flame spread along a linear fuel droplet array with pre-vaporization in microgravity [7].

Figure 1 shows the schematic concept of the combustion

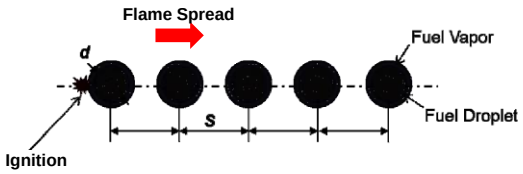

Fig. 1 Schematic concept of the combustion experiment.

1 Japan Aerospace Exploration Agency (JAXA) 2-1-1 Sengen, Tsukuba, Ibaraki 305-8505, Japan.
2 IIC Co. Ltd. 1-100 Takamatsu, Tachikawa, Tokyo 190-0011, Japan.
3 Japan Aerospace Exploration Agency (JAXA) 3-1-1 Yoshinodai, Chuo-Ku, Sagamihara, Kanagawa 252-5210, Japan.
4 Japan Aerospace Exploration Agency (JAXA) 7-44-1 Jindaiji Higashimachi, Chofu, Tokyo 182-8522, Japan.
5 A.E.S. Co. Ltd. 1-6-1 Takezono, Tsukuba, Ibaraki 305-0032, Japan.
(E-mail: Corresponding.Author kikuchi.masao@jaxa.jp)

 ©2015 The Jpn. Soc. Microgravity Appl.

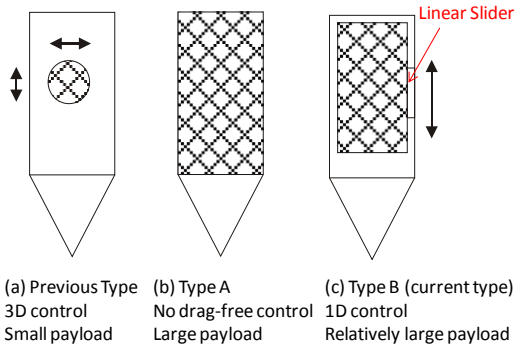

Fig. 2 Comparison of drag-free control methods of the payload

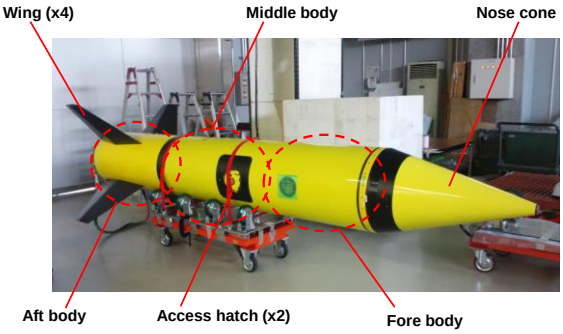

Fig. 3 Appearance of the balloon operated vehicle

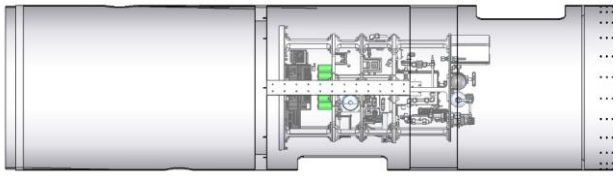

Fig. 4 Microgravity experiment module in the middle body

experiment. Similarly to the TEXUS rocket experiment, the observation of flame spread phenomena along n-decane droplet array in 500 K air was planned in this current experiment. In the TEXUS rocket experiment, flame spread with relatively large degree of pre-vaporization was observed three times by varying the pre-vaporization time during the 6 minutes microgravity period[6]. However, one observation of flame spread with a relatively small degree of pre-vaporization was intended during the current 30 s microgravity experiment. It was expected that data obtained by the balloon experiment could fill the gap between those taken by the short duration drop tower/shaft experiments and the longer duration TEXUS rocket experiments.

3. Experimental System

The differences of drag-free control methods in the previous and the current systems are indicated in **Fig. 2**. In the previous system (**Fig. 2(a)**), the three dimensional (3D) relative position of the inner capsule (the microgravity experiment section) was

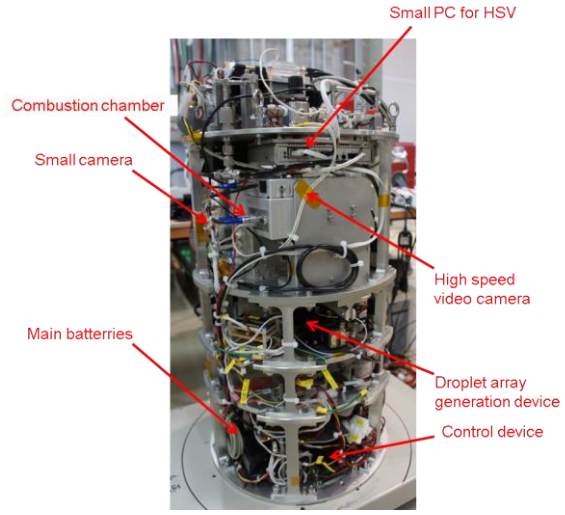

Fig. 5 Overview of the modified DCU for the balloon experiment.

measured from the outer capsule, and the cold gas jets in the outer capsule produced forces to cancel the disturbances and kept the distance between the inner and outer capsule constant. Although the 3D control method offered high quality microgravity environment during the free-fall of the BOV, the payload shape was limited to that of a sphere with a size not larger than 28 cm in diameter.

A free-fall capsule without a drag-free system (shown in **Fig. 2 (b)**) was tested in 1983, and low gravity environment with 2.9 x 10^{-3} G was obtained for 10 s [8].

In the current system (**Fig. 2(c)**), a one dimensional (1D) drag-free control system using a linear slider mechanism was adopted. The payload and the outer capsule (balloon operated vehicle) were mechanically connected by the linear slider. When the vertical distance between the payload and the vehicle decreased by drag force to the vehicle, longitudinal cold gas jet thrusters at the rear end of the vehicle were activated so that they cancelled disturbances and maintained appropriate distances between the payload and the outside the vehicle. Better gravity levels (as low as 10^{-3} G) and longer durations (as long as 30 s) were expected with this system compared to devices without any drag-free control (**Fig. 2(b)**).

As a result, the allowable payload size could be enlarged to 400 mm in diameter and 600 mm in height. The payload weight could also be increased from 15 kg to 50 kg.

Figure 3 shows the BOV on the ground. The shape of the vehicle (outer capsule for the payload) is almost identical to that of the previous system. The total length of the vehicle is about 4.1 m and the outer diameter of the body is about 0.6 m. The weight of the vehicle including the microgravity experiment module is about 310 kg. The vehicle consists of a nose cone, a fore body, a middle body, and an aft body with four wings. The fore body and the middle body accommodate vehicle support

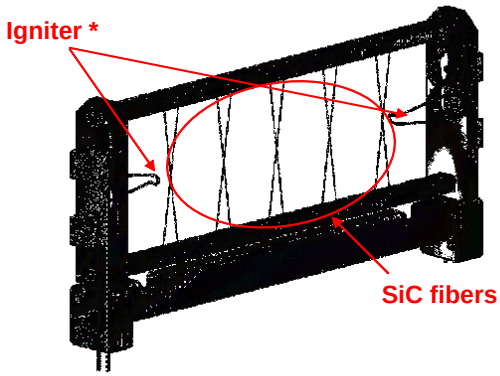

Fig. 6 Schematic of the droplet array holder (*only 1 igniter was installed in the current experiment)

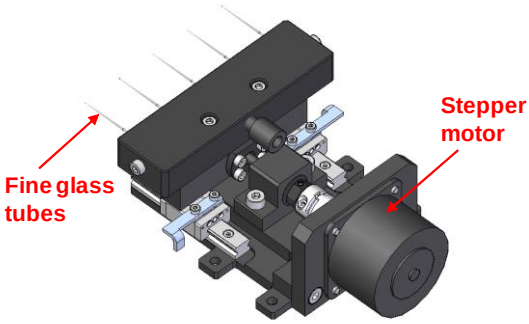

Fig. 7 Schematic of the droplet array generation device

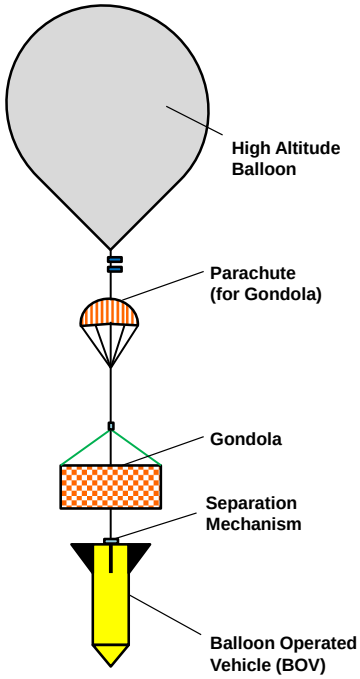

Fig. 8 Schematic drawing of the whole configuration of the balloon experiment system

devices as well as the payload whereas the aft body houses the parachute of the vehicle and the cold gas jet thrusters. The fore body and the middle body are airtight structures, so that the inner pressure is kept at atmospheric pressure (about 1 atm) even at higher altitude. Also, the structures protect the inner devices from sea water after splashdown. Detailed position of Microgravity experiment module in the middle body is shown in **Fig. 4**.

Figure 5 shows the modified EM of the DCU employed as the payload for the current experiment. The weight of the payload is about 50 kg. Although the control device and batteries for the payload were provided by the rocket side in the TEXUS experiment, the whole system had to be integrated to the payload itself in the current BOV system. Therefore, control devices and batteries were added in the experimental apparatus. Also, observation devices including a high-speed video camera were replaced with smaller ones.

In the current experiment, experimental devices for fuel droplet array generation similar to those of TEXUS rocket experiment were employed. The droplet array holder was composed of five sets of X-shaped SiC fibers with 14 μm diameter to support fuel droplets on intersections of the fibers **(Fig. 6)**. Only one igniter was installed in the current experiment while 2 igniters were installed in the TEXUS experiment.

In TEXUS experiment, four combustion runs were planned during about 6 minutes of microgravity duration. If the nominal igniter had some trouble during the flight, it was planned to employ a spare igniter for the subsequent combustion runs. However, only one combustion run was possible for the current experiment. Therefore, only one igniter was installed in the current system.

Droplet array generation system generates droplets on intersections of SiC fibers by supplying fuel from the tips of fine glass tubes, as shown in **Fig. 7**. n-Decane ($C_{10}H_{22}$) was employed as fuel in the flight experiment, just as in the TEXUS experiment. The combustion chamber, equipped with electric heaters, is also the same as that of the TEXUS experiment.

A triaxial accelerometer (Silicon Design Inc. Model 2440) was set in the DCU to measure the gravity level. The output signals of the accelerometer were recorded in a data logger (RHOM-Riken R2-Micro) with a 900 Hz sampling rate.

The whole experimental system is shown in **Fig. 8.** It consists of the high altitude balloon, the gondola, the BOV, and the payload inside the BOV. It was possible to lift scientific payloads weighing 700 kg to an altitude of 40 km with the high altitude balloon filled with helium gas. The BOV was lifted up by the balloon via the gondola. All the operation devices necessary to control the high altitude balloon, including ballast, computers, electrical batteries, and communication devices were accommodated in the gondola. Two small secondary payloads were also housed in the gondola. Maximum height of these systems was beyond 150 m.

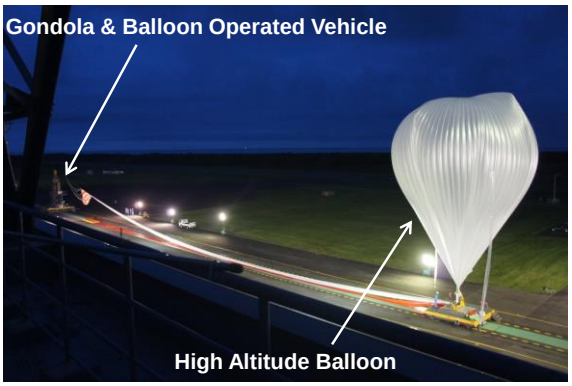

Fig. 9 Whole view of the high altitude balloon, the gondola and the balloon operated vehicle before the release

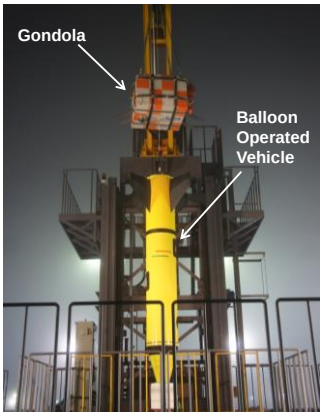

Fig. 10 The gondola and the balloon operated vehicle at the launch pad

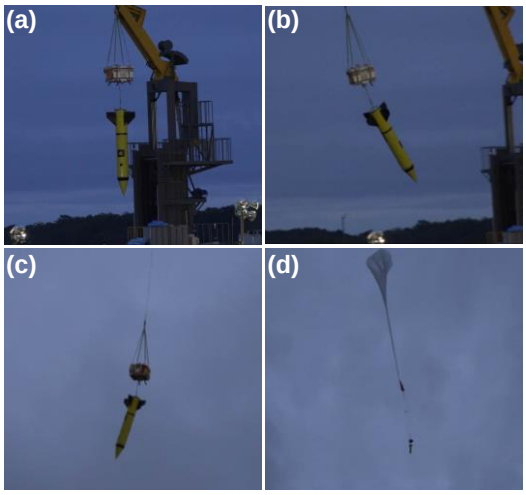

Fig. 11 Sequential photos of the balloon operated vehicle after the release of the balloon

4. Result of the Experiment

4.1 Flight operations

Final ground operation at the TARF for the BOV flight experiment started at about 23:30 on August 21st. Power system, control system, and communication system of the vehicle were turned on and every access hatches of the vehicle body were closed. Confirmations on transmission and reception conditions of the telemetry signals and tele-commands were performed between the vehicle and the ground system. After the preparation of the vehicle was completed, injection of helium gas to the balloon was started at around 3:00 on August 22nd. Finally, the balloon with the vehicle was released to air at around 4:30. Photos of the balloon and the vehicle during the final preparation phase are shown in **Fig. 9** and **Fig. 10**. Also, sequential photos of the vehicle at the moment of the balloon release are shown in **Fig. 11.**

During ascent of the balloon, several tele-commands for experiment preparation were sent to the vehicle from the ground. Heating of the combustion chamber was started at around 5:50. Temperature inside the combustion chamber increased to 500 K within 45 minutes, the same as that for nominal ground tests. The balloon reached an altitude of 38 km at around 7:00. Five minutes prior to the free-fall (release of the vehicle from the gondola), an automatic timer sequence of the experiment procedures was started. The vehicle was released from the gondola at 7:11. Sequential photos of the vehicle after the release, obtained by video camera at the gondola, are shown in **Fig. 12**.

From the onset of the free fall, experiment sequences of the payload such as generation of n-decane droplet array on the array holder, insert of the array holder into the combustion chamber, ignition after 3 s pre-vaporization, and recording of video images by cameras were automatically performed. About 35 s later, pilot parachute at the rear end of the vehicle was deployed and free fall of the vehicle was terminated. Also, about 320 s after the onset of the free-fall, the main parachute was deployed from the vehicle. The vehicle splashed down into the sea at around 7:27 after which the vehicle as well as the gondola and balloon were retrieved by ships.

After the retrieval of the vehicle, the experimental data including high-speed video camera and backlit camera images were retrieved. Measured data such as temperature, humidity as well as gravity level in the microgravity module, were also successfully retrieved.

4.2 Gravity level

Figure 13 shows the measured acceleration data as a function of time in the microgravity module during the free-fall. The Z-axis indicates the longitudinal direction along the vehicle body, while X and Y-axis indicate the lateral directions. In **Fig. 13**, the onset of the free-fall was set to be 0 s. After 4 seconds from the free-fall, the acceleration was gradually reduced. Some spike-like disturbances shown in 13 s and 27 s were introduced by the combustion experiment apparatus during the

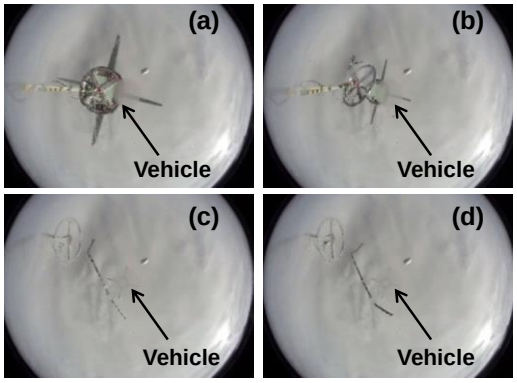

Fig. 12 Sequential photos of the vehicle after the release from the gondola

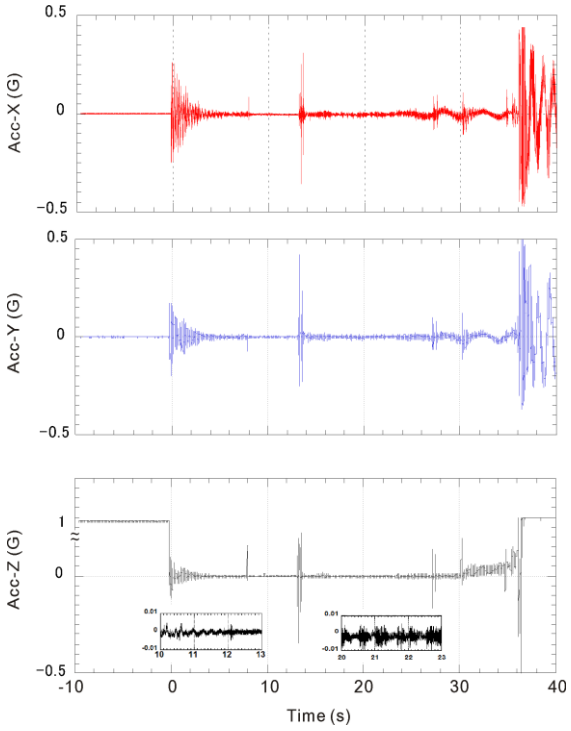

Fig. 13 Measured acceleration data in the microgravity module

insertion/removal of the array holder into/from the combustion chamber. Low gravity level was obtained during 8 to 13 s. After 13 s, the gravity level was gradually increased due to the increasing air friction on the outer capsule, even though the gas jet thrusters tried to cancel it. At around 25 s, a wavy behavior in the acceleration signal can be observed in the X and Y directions, which indicates that the vehicle started slightly wobbling. After 35 s, low gravity conditions were terminated due to the deployment of the parachute.

Figure 14 shows the obtained low gravity level as a function of frequency. In this frequency-domain analysis, the acceleration data from 0 to 30 s were used. According to the figure, the gravity level of the payload was less than 10^{-3} G in low

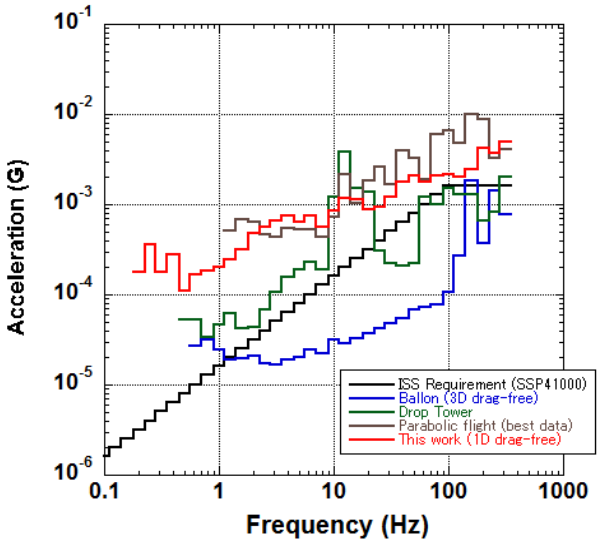

Fig. 14 Result of frequency band analysis and comparison of gravity level among other flight opportunities

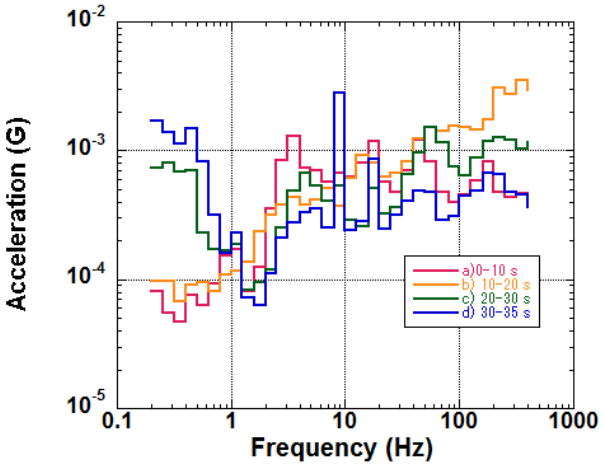

Fig. 15 Change of gravity level in the first balloon experiment

frequency region (less than 100 Hz). This confirmed that the new system with one dimensional drag-free control can provide a good low gravity condition (as low as 10^{-3} G) for 30 seconds.

The frequency analyses with four different time frames; a) 0 to 10 s, b) 10 to 20 s, c) 20 to 30 s, and d) 30 to 35 s, are shown in **Fig. 15**. From the comparison between data a) and b), it can be seen that the acceleration levels at high frequency (more than 50 Hz) were increased from 10 to 20 s. Based on the fact that drag-free control by gas jet thrusters became fully operational from 13 s, these high frequency disturbances were introduced mainly by the gas jet thrusters. However, the comparison between b), c), and d), reveals a significant increase of acceleration level at low frequency (less than 1 Hz). This disturbance at low frequency was attributed to the air friction.

Comparison of gravity level with other low gravity system is shown in **Fig. 14.** Even though the gravity level is higher than that of 3-dimensional drag free control system, the new system

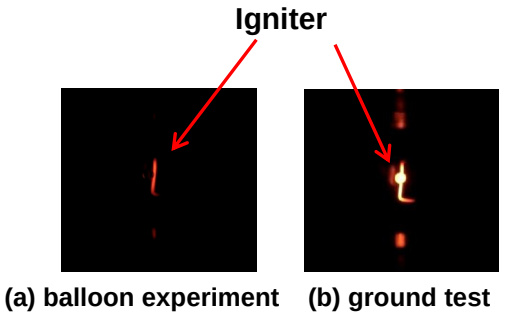

Fig. 16 Comparison of the glowing igniters

can provide better and longer gravity levels than those offered by parabolic flights.

4.3 Combustion experiment

As for the combustion experiment with the payload, the activation of the igniter (Fe-Cr wire) was confirmed from video images obtained at nominal timing. However, ignition of the n-decane droplet did not occur. **Figure 16** shows the igniter which was glowing due to electric current during the experiment. The brightness of the igniter was lower than that observed in the ground tests. Also, the time length of glowing was shorter than that measured in the tests. After the retrieval of the DCU, every component was checked, and no problem was found. **Figure 17** shows the history of temperature in the DCU. During the ascent of the balloon, the temperature went down below the dew point (16ºC, which has been determined from the humidity (72% RH) and temperature (23ºC) when the access hatches were closed). After troubleshooting activities, it was confirmed that the dew condensation on the igniter caused this trouble. The humidity inside the BOV should have been minimized.

5. Summary

The flight experiment by the balloon operated vehicle was performed at the JAXA's Taiki Aerospace Research Field (TARF) in the summer of 2014. The primary objective of the flight experiment was to demonstrate and verify the capability of a new drag-free system for microgravity experiment. Also, combustion experiment on flame spread of n-decane droplet array was intended. The whole flight experiment including the retrieval of the vehicle was successfully performed. According to the obtained data, it was confirmed that the vehicle with the new drag-free system successfully achieved low-gravity environment in the order of 10^{-3} G for more than 30 s. Regarding the combustion experiment, ignition of the fuel droplet did not occur due to insufficient glowing of the igniter.

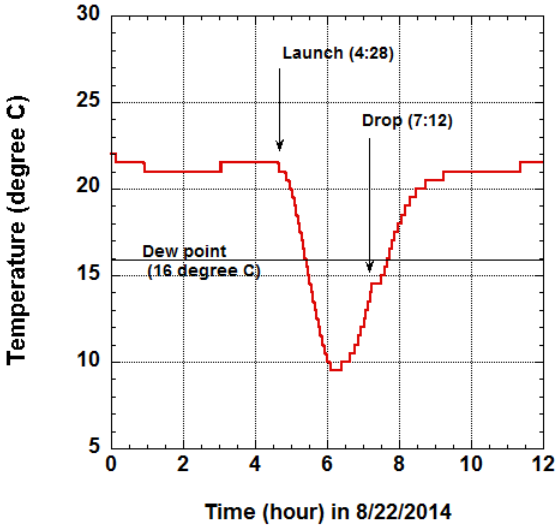

Fig. 17 History of temperature around igniter in the DCU.

Acknowledgments

Authors are grateful to the JAXA balloon launch operation staff for their dedicated work at TARF as well as their help and useful comments during preparation.

References

1) T. Hashimoto, S. Sawai, S. Sakai, N. Bando, H. Kobayashi, T. Ishikawa, Y. Inatomi, K. Fujita, T. Yoshimitsu, Y. Saito, and H. Fuke: J. Jpn. Soc. Microgravity Appl., **26** (2009) 9.
2) T. Ishikawa, Y. Inatomi, T. Hashimoto, S. Sawai, Y. Saito, T. Yoshimitsu, S. Sakai, H. Kobayashi, K. Fujita, N. Bando, and M.Goto: J. Jpn. Soc. Microgravity Appl., **25** (2008) 3.
3) S.Sawai, T. Hashimoto, S. Sakai, N. Bando, H. Kobayashi, T. Yoshimitsu, T. Ishikawa, Y. Inatomi, H. Fuke, Y. Kamata, S. Hoshino, K. Tajima, S. Kadooka, S. Uehara, T. Kojima, S. Ueno, K. Miyaji, N. Tsuboi, K. Hiraki, K. Suzuki, K. Matsushima, and T. Nakata: JSASS, **56** (2008) 339.
4) T. Ishikawa, T. Hashimoto, S. Sawai, Y. Saito, Y. Inatomi, T. Yoshimitsu, S. Sakai, H. Kobayashi, K. Fujita, and N. Bando: Transaction of JSASS Space Tech. Japan, **7** (2009) 29.
5) T. Ishikawa, M. Kikuchi, S. Yamamoto, S. Sawai, Y. Maru, T. Hashimoto, S. Sakai, N. Bando, S. Shimizu, H. Kobayashi, T. Yoshimitsu, Y. Kan, A. Tazaki, S. Fukuyama, J. Okada, S. Yoda, H. Fuke, and Y. Kakehashi: Proc. FY24 Balloon Symposium, 2012, isas-12-sbs-023. (in Japanese)
6) M. Kikuchi, S. Yamamoto, M. Mikami, H. Nomura, O. Moriue, and A. Umemura: Proc. 49th Combustion Symposium, 2011, p.108. (Japanese)
7) M. Kikuchi, T. Ishikawa, S. Yamamoto, Y. Maru, N. Bando, Y. Kan, A. Tazaki, S. Fukuyama, J. Okada, and H. Fuke: Trans. JSASS Aerospace Tech. Japan, **12** ists29 (2014) Th_19.
8) M. Namiki, S. Ohta, T. Yamagami, Y. Koma, H. Akiyama, H. Hirosawa and J. Nishimura: Adv. Space Res., **5** (1985) 83.